Received: 21 September 2021 | Revised: 2 February 2022 | Accepted: 4 February 2022

DOI: 10.1002/arp.1857

RESEARCH ARTICLE

WILEY

Capabilities and limitations of electrical resistivity tomography for mapping and surveying hillfort fortifications

Radek Klanica[1] | Roman Křivánek[2] | Hana Grison[1] | Petr Tábořík[3] | Jindřich Šteffl[4]

[1]Institute of Geophysics, Czech Academy of Sciences, Prague, Czech Republic

[2]Institute of Archaeology, Czech Academy of Sciences, Prague, Czech Republic

[3]Faculty of Science, Institute of Hydrogeology, Engineering Geology and Applied Geophysics, Charles University, Prague, Czech Republic

[4]Department of Archaeology, Regional Museum in Teplice, Teplice, Czech Republic

Correspondence
Radek Klanica, Institute of Geophysics, Czech Academy of Sciences, Boční II/1401, Prague 4, Czech Republic.
Email: rk@ig.cas.cz

Funding information
Univerzita Karlova v Praze, Grant/Award Number: UNCE/SCI/006; Ministerstvo Školství, Mládeže a Tělovýchovy, Grant/Award Number: LTC19029

Abstract

Hillforts are fortified archaeological sites built from the Neolithic to Early Middle Ages within the area of Europe. They were usually surrounded by fortifications consisting of various combinations of ramparts and ditches, which today constitute their most striking remains. Although magnetometry surveys are commonly used for spatial identification of ramparts and ditches, a different method must be employed for directly obtaining depth information. Hence, we evaluate the potential of electrical resistivity tomography (ERT) for surveying hillfort fortifications. Within three hillforts of different ages in the Czech Republic, we investigated various features affecting the imaging ability of ERT, including bedrock type, building material, present-day condition of fortification, impact of past or recent agricultural activities, and field settings of the ERT method. Supported by additional information from magnetometry and electromagnetic surveys, the results show that ERT is most applicable in cases of stony ramparts, ditches carved into rocky bedrock or well-preserved earthen ramparts. Poorer results were achieved upon active and/or recently active agricultural lands, where fortifications have been gradually destroyed by ploughing. The remains of stony ramparts remained distinguishable in the latter case, but mere traces of earthen ramparts and ditches were invisible to ERT due to mixing of fortification material with on-site soil. ERT is a unique method for detailed investigation of both ramparts and ditches by which a structure and its extent can be evaluated to indicate the function of a settlement and obtain information about former environmental conditions, population, land use and/or human–environmental interaction.

KEYWORDS
ditch, electrical resistivity tomography, fortification, hillfort, magnetometry, rampart

1 | INTRODUCTION

Hillforts are fortified archaeological sites spread throughout Europe, including within the territory of the Czech Republic, that were built from the Neolithic to the Early Middle Ages (Čtverák et al., 2003). These sites were preferentially established at strategic places protected by natural elements, such as on mountains and hills bordered by steep slopes or watercourses. The hillforts served for various purposes, including strategic, cultural and religious (Vencl, 1984). Due to the builders' limited construction abilities, and especially of inhabitants from earlier ages, only ramparts and ditches have been preserved to the present day. These fortified structures usually surround and/or divide the hillfort area and are today the most investigated phenomena related to hillforts.

Hillfort fortifications exist in numerous shapes and sizes, depending upon the age of origin, location, time of occupation and

importance of a given site. In general, and probably serving for defensive purposes, there would be huge ditches several metres deep accompanied by ramparts, palisades and/or stone walls, possibly including more complex constructions consisting of two or three ditches and/or ramparts in succession (e.g., Christensen, 2004; Osgood et al., 2000). Considerably, smaller ditches or isolated ramparts without ditches might delineate hillforts built only for special purposes, such as cultural, religious or astronomical (e.g., Oliva, 2004; Parkinson & Duffy, 2007; Zotti & Neubauer, 2011), but an absence of more complex fortification can be related also to the terrain situation at a given site or to a region or cultural period. From the infill of sunken features (including ditches), information can be retrieved about former environmental conditions, the population of settlement or human–environmental interaction.

Hillfort fortifications can be detected by various techniques, including satellite imaging, aerial photography, LiDAR sensing and geophysical prospection (e.g., Oswin, 2009; Wiseman & El-Baz, 2007). Whereas geophysical methods can image a variety of archaeological features in the subsurface, magnetometry surveys have a special place in archaeological prospection. The materials found at archaeological sites often contain iron oxides, while past exposure of these materials to intense heat usually resulted in detectable magnetic anomalies (for detailed principles, see, e.g., Fassbinder, 2017). Thus, magnetometry surveys are commonly used for detecting features associated with burning, such as hearths, kilns or cooking pits (e.g., Andreou et al., 2017; Urban et al., 2014, 2019). Magnetometry is also used for detecting ramparts (e.g., Hegyi et al., 2018), because they were in many cases vitrified (i.e., burned out by fire), thus resulting in strong thermoremanent magnetization (e.g., Catanzariti et al., 2008). The infill of former ditches usually has different magnetic properties than do the surrounding soils and thus can be identified usually as linear (oval or irregular) magnetic anomalies with different magnetization (e.g., Schultze et al., 2008) due to enhanced magnetic susceptibility of archaeological matter (e.g., Le Borgne, 1960; Mullins, 1977) or natural remanent magnetization (Fassbinder & Stanjek, 1993). Unfortunately, magnetometry surveys are almost unusable in cases of igneous bedrock or in the presence of human metallic infrastructures, whereby archaeological magnetic anomalies are hidden under stronger magnetic signal of natural and/or human origin.

Although magnetometry survey is ideal for spatial recognition of former fortification remains, it is almost inapplicable for obtaining vertical information (i.e., depth of the ditches or thickness of ramparts). A more suitable method must be employed for this task, such as electrical or electromagnetic methods or detailed magnetic susceptibility measurements. Electrical resistivity tomography (ERT) uses an injection of electric current into the ground through two current electrodes (C1 and C2) while measuring electrical potential between another two potential electrodes (P1 and P2) and subsequent calculation of apparent electrical resistivity according to Ohm's law. Then, apparent resistivity must be transformed to real resistivity by inversion, by which an inversion program seeks to find a resistivity model explaining the measured data. By changing of different current and potential pairs of electrodes, ERT characterizes subsurface distribution of electrical resistivity in both lateral and vertical directions (e.g., Loke, 2020; Loke & Barker, 1996; Tabbagh, 2017), and thus, fortifications can be distinguished from the surrounding environment. It is widely used in archaeology for a variety of situations, including to investigate graves (e.g., Nero et al., 2016), building foundations (e.g., Al-Saadi et al., 2017), walls (e.g., Leontarakis & Apostolopoulos, 2013) and burial mounds (e.g., Zhao et al., 2019). Although ERT also has been used for mapping of hillfort fortifications (e.g., Nowaczinski et al., 2012), the extent of such use is surprisingly small and especially in the case of ditches. Hillfort ramparts could be stacked from massive, low porosity and thus resistive stones; built with combinations of wood, earth and stones with mid-range resistivity; or have the form of a low-resistivity earthen wall. In general, the ditches manifest low resistivities due to their infill by sediments, which further reduce resistivity due to their greater moisture retention. Unlike magnetometry surveys, ERT is not sensitive to magnetic properties and thus can be used even on igneous bedrock. Due to its field set-up in a single line, ERT's measurements can be taken at sites posing various levels of difficulty, and it also is very resistant to any sources of artificial noise. ERT is not ideal in efficiency terms for spatial survey, because areal 3D survey is extremely demanding of time and human resource.

In providing direct vertical information, electromagnetic methods, such as ground penetrating radar (GPR) or frequency-domain electromagnetic survey (FDEM), can be employed. Both ramparts and ditches can be imaged by GPR (e.g., Hegyi et al., 2018), but, because it was not used in our study, it will not be further discussed (more information about GPR in archaeological prospection can be found in, e.g., Goodman & Piro, 2013). The FDEM method works on the principles of electromagnetic induction, whereby a time-varying electromagnetic field is generated by a transmitter coil and an induced electromagnetic field is recorded by a receiver coil. The received signal consists in two components: in-phase and out-of-phase with the transmitted signal. These components are (under low induction number) related to apparent magnetic susceptibility and bulk apparent resistivity (e.g., Di Maio et al., 2018; Tabbagh, 2017). FDEM surveys are usually used in combination with other methods for identification of building foundations (e.g., Di Maio et al., 2018) and ditches (e.g., Simpson et al., 2010) or for archaeological site prospection generally (e.g., de Smedt et al., 2013; Rodrigues et al., 2009). FDEM survey offers a combination of both magnetic and resistivity information, but, due to its dependency on the principles of EM induction, it cannot be used in the vicinity of such human-made conductive structures as pipelines or electric fences.

The main aim of this paper is to evaluate the potential of ERT for hillfort fortification surveys while considering different types of bedrock and pedological properties, present conditions of fortifications (and also their construction material), impact of agricultural activities and ERT field settings, including selection of array type and electrode spacing. The results are presented and discussed for three hillforts of different ages within the Czech Republic (Figure 1) and with supportive information from other archaeogeophysical measurements (i.e., magnetometry and FDEM surveys).

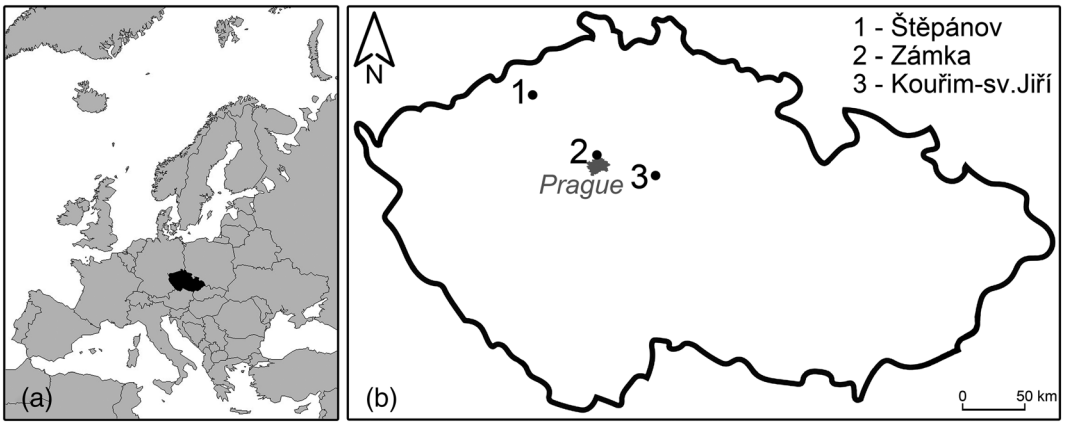

FIGURE 1 (a) Schematic map of Europe with position of the Czech Republic and (b) position of studied hillforts within the Czech Republic

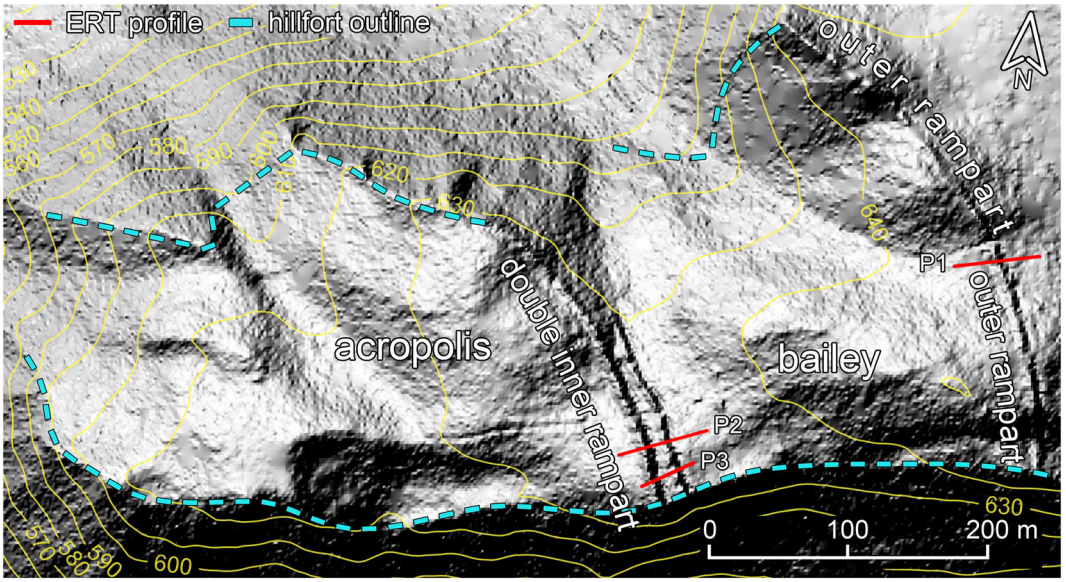

FIGURE 2 Topographic map of the hillfort Štěpánov based on a LiDAR digital elevation model (CUZK, 2017), with measured ERT profiles [Colour figure can be viewed at wileyonlinelibrary.com]

2 | GEOLOGICAL AND ARCHAEOLOGICAL SETTINGS OF STUDIED SITES

2.1 | Hillfort Štěpánov

The hillfort Štěpánov is situated on the top of Štěpánov Hill (651 m a.s.l.) belonging to the České Středohoří Mts. volcanic–sedimentary complex composed of an assemblage of Tertiary alkaline volcanics and sediment intercalations. Štěpánov Hill is composed of alkaline basalt of the Ústí Formation (ca. 36–26 Ma), and near the surface, it has been eroded into rocky and rubble fields (Cajz, 2000). The compact basaltic bedrock is expected to occur very near to the surface. The igneous bedrock is highly magnetic, preventing use of magnetometry surveying for archaeological purposes.

The hillfort area encompasses the top of the hill with an adjacent promontory, constituting the southernmost part of the Pařez massif (736 m a.s.l.). The promontory is oriented east–west, is slightly sloped from north-east to south-west (Čtverák et al., 2003) and ranges in altitude between 620 and 651 m a.s.l. Steep slopes on the northern, western and southern sides naturally protect the hillfort area, while the elevation difference from the surrounding landscape is between 110 and 150 m.

The total area of the hillfort is 12 ha, and it is divided into two parts: the acropolis and the outer bailey, each covering 6 ha (Figure 2). The fortification was built on the eastern side, thereby separating the promontory with the hillfort from the rest of the Pařez massif. Fortification structures include (from bailey to acropolis) a ditch with outer transverse rampart delimiting the outer bailey and an inner double rampart with two ditches between the bailey and acropolis, arranged as follows: ditch–rampart–ditch–rampart (Smrž, 1995).

The outer rampart is ~400 m long and can be divided into southern and northern parts. The southern part has a ditch ~0.45 m deep

along its full length, the rampart itself is 0.65 m high (from the bailey), and total fortification width including both ditch and rampart is ~10 m. The northern part lacks the ditch in the last 100 m, and the rampart is 2.7 m high (from the bailey), while its total width is 17.5 m around that area. The inner double rampart consists of two ramparts: an outer rampart 143 m long and an inner rampart 246 m long. The present total width of the fortification system, where both ramparts are present, is ~30 m, while the height of the outer rampart is 2.5 m and the inner rampart almost 3 m. The remnants of ditches where they existed are around 0.7 to 0.9 m deep.

Although the hillfort area has not been extensively investigated, metal and ceramic artefacts have been found that allow dating the settlement to the Late Bronze Age (1000 to 750 BC). This period is suggested especially by the presence of bronze objects (knives, sickles and axes) and ceramic material (mostly settlement related).

2.2 | Hillfort Zámka

The hillfort Zámka spreads out above the right bank of the Vltava River, north of Prague within the Proterozoic Kralupy–Zbraslav Group composed of greywackes and siltstones covered by Quaternary loess. The hillfort lies on a distinct promontory (highest point 251 m a.s.l.) elongated in an east–west direction and protected by narrow valleys from the north and south. The western side is bounded by the Vltava River. The difference in elevation from the Vltava River and adjacent valley floors reaches up to 60 m.

The prehistoric hillfort covers a promontory with an area of about 6.5 ha and was protected from the eastern side by a rampart with ditch (Figure 3). The rampart was built using a combination of earth, stones and wood and probably was burnt out by fire (Čtverák et al., 2003). There is a ditch on the eastern side. Due to intensive agricultural activities and recent landscaping, the remains of the fortification have today the form of an indistinct terrain rise with ~2 m height and 50 m width. The total hillfort area, including baileys from the Middle Ages (at which time the prehistoric core was used as an acropolis), extends to 12 ha (Křivánek, 2008, 2013).

The promontory was inhabited from the Eneolithic (3800–3400 and 3100–2800 BC) through the Bronze Age (2300–800 BC) and Iron Age (800–400 BC) up to the Early Middle Ages (500–900 AD), as suggested by excavations. The main fortification structure was probably established at the turn of the eighth and ninth centuries (Kudrnáč, 1963), and the hillfort was abandoned at the end of ninth century with onset of the Přemyslid dynasty (Mašek & Fridrichová, 1965; Profantová, 1996).

2.3 | Hillfort Kouřim-sv. Jiří

The hillfort Kouřim-sv. Jiří was built within the Kutná Hora Crystalline, here represented by two-mica migmatites to orthogneisses, which are covered by aeolian Quaternary loess. The hillfort lies south of the town of Kouřim on a promontory (highest point 281 m a.s.l.) above the confluence of two small streams that border the promontory from the west, north and east with ~30 m of elevation difference.

The hillfort area encompasses ~9 ha and is divided into three parts: northern bailey; acropolis (with castle and church); and outer, southern part (Figure 4, Tomanová, 2012). The northern bailey and acropolis were surrounded by an outer rampart built of earth and wood with total width ~10–12 m, reinforced by a frontal wall of piled stones around 2.5 m wide. The remains of a ditch were found only on the southern side. The outer fortification line is situated today upon active agricultural land, an indistinct terrain rise ~1.5 m high and 40 m wide. A better preserved part of the rampart within a grove of trees is ~3 m high and

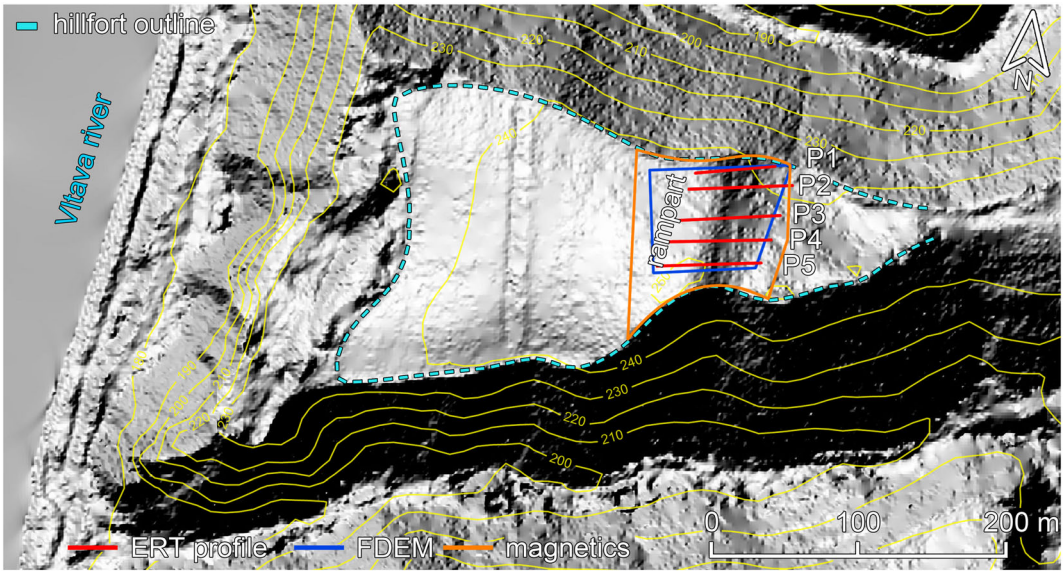

FIGURE 3 Topographic map of the hillfort Zámka based on a LiDAR digital elevation model (CUZK, 2017), with placement of the geophysical surveys [Colour figure can be viewed at wileyonlinelibrary.com]

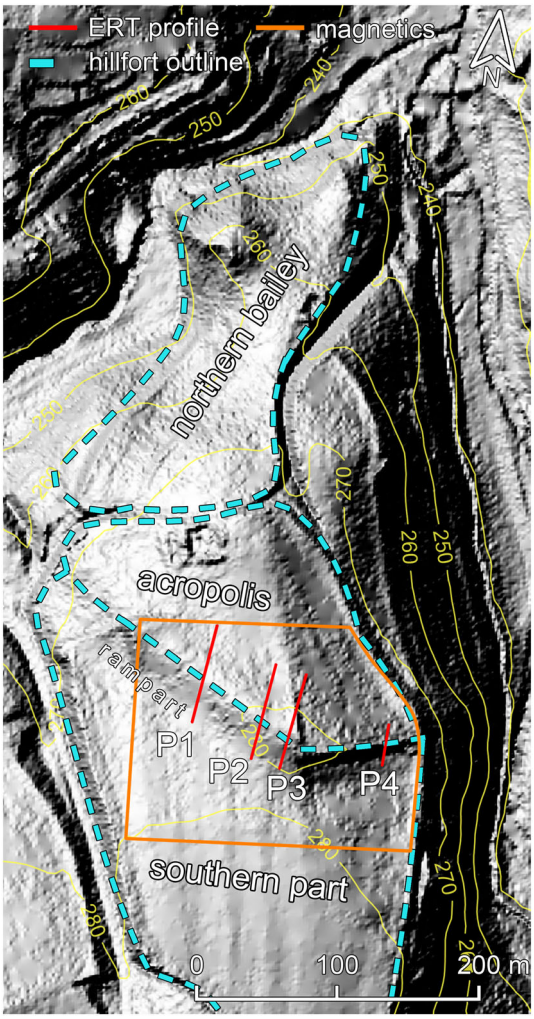

FIGURE 4 Topographic map of the hillfort Kouřim-sv. Jiří based on a LiDAR digital elevation model (CUZK, 2017), with measured ERT profiles and magnetometry survey [Colour figure can be viewed at wileyonlinelibrary.com]

15 m wide. Later, an inner rampart with a ditch between the northern bailey and acropolis (unpreserved today) was also built. The rampart was made of earth with a frontal stone wall, and the total width of the fortification was 8 to 9 m (Šolle, 1969, 1993, 2000).

As suggested by excavations, the hillfort area was inhabited from the Iron Age (600–500 BC) through the Early Middle Ages (ca. 8th century), but its main prosperity relates to the Přemyslid dynasty within the 10th to 13th centuries, when the main fortifications together with a castle and church were also built. The hillfort was conquered and destroyed in 1223 (Tomanová, 2012).

3 | GEOPHYSICAL METHODS

Although the main goal of this study is to evaluate the applicability of ERT, results from other methods were used also on those sites located on agricultural land to provide supportive information from different geophysical methods (magnetometry and FDEM surveys; for summary of field works, see Table 1). All ERT profiles were measured using the five-channel ARES II resistivity system (GF Instruments, Brno, Czech Republic) with several different electrode arrays within each locality (Wenner–Schlumberger [WS], inverse Wenner–Schlumberger [IWS; regular WS array with switched current and potential electrodes] and dipole–dipole [DD]). For sketches and advantages of the individual electrode configurations, see, for example, Dahlin and Zhou (2004), Loke (2020) and Section 3.2.1. All arrays were used in a high-density (HD) arrangement with a larger number of measured points than in the cases of regular arrays of the same type. This is done by using overlapping data levels with different combinations of distances between C1–C2 and P1–P2 electrodes. The total number of data points acquired by such configuration is approximately double than those obtained by a regular non-HD array (Loke, 2020). Within selected hillforts, tests of electrode array and electrode spacing were performed (see Section 3.1). Rainfall and soil moisture effects on ERT data were neglected, because significant seasonal changes of soil moisture are usually observed to depth ~0.90 m (de Jong et al., 2020), but the shallowest data with 1 m electrode spacing were collected from depth of 0.60 m. Thus, soil moisture most likely does not affect results on metre-sized and thick and/or deep defensive structures. Magnetometry surveys were measured by a Scintrex SM-4G caesium magnetometer (Scintrex, Concord, ON, Canada) registering the vertical gradient of total magnetic field. The FDEM survey utilized a CMD-Explorer three-depth probe (GF Instruments) with dipole centre distances 1.48/2.82/4.49 m in low depth range setting (horizontal orientation of coils) related to calibrated depth levels 1.1/2.1/3.3 m.

ERT data were processed using the Res2Dinv algorithm (Loke & Barker, 1996; for details of inversion routine, see, e.g., Loke, 2020), with topographic correction based on a LiDAR digital elevation model (CUZK, 2017). Hillfort Štěpánov was inverted using the L1 norm (so-called robust inversion), due to an expected sharp resistivity boundary between the rampart and rocky basement, while hillforts Zámka and Kouřim-sv. Jiří were inverted by the L2 norm (standard inversion; for use of different norms, see, e.g., Loke et al., 2003) favouring smooth transitions as expected within ploughed fields. All geophysical data sets, including the final inverse models, were interpolated and visualized in Surfer (Golden Software, Golden, CO, USA).

3.1 | Field works

3.1.1 | Hillfort Štěpánov

Two ERT profiles (P1 and P2) were measured within the hillfort fortifications, both with 1 m electrode spacing and using a WS HD electrode array. The profile across the outer transverse rampart was 55 m long, and length of the profile crossing the inner double rampart was 71 m. In addition, one profile 40 m long (P3) using an IWS HD electrode array across the inner double rampart was measured in order to test resolution differences in output among individual electrode spacings (0.5/1/2/4 m; Figure 2).

TABLE 1 Summary of field works

	Electrical resistivity tomography				
Site	**Profiles**	**Array**	**Electrode spacing**	**Magnetics**	**FDEM survey**
Štěpánov	3	WS/IWS HD	0.5/1/2/4 m	/	/
Zámka	5	WS/DD HD	1 m	x	x
Kouřim-sv. Jiří	4	WS/IWS/DD HD	1 m	x	/

3.1.2 | Hillfort Zámka

Previous geophysical study of the hillfort area included detailed magnetometry survey during 2005–2006. Data were collected in a regular 1 × 0.25 m grid, covering both the prehistoric part of the hillfort on the promontory and the Middle Ages bailey (Křivánek, 2008, 2010, 2013). Spatial results from the magnetogram were used for efficient placement of the ERT profiles and FDEM survey. Within this study, only the results from the vicinity of the fortification are presented.

Five parallel ERT profiles (P1–P5), with ∼15 m north–south offset, were measured on Zámka. While P1 was 55 m long, the others had the same 71 m length. All profiles used electrode spacing of 1 m (Figure 3) and were obtained using a WS HD electrode array, while on P1 and P2, the DD HD array was also tested.

In addition, a zone of the former rampart and ditch was supplemented with the FDEM survey covering a polygon of 0.57 ha (roughly based on a 71 × 71 m^2). It covered three depth levels (1.1, 2.1 and 3.3 m) and was performed as east–west profiles in continuous mode with sampling frequency of 10 Hz and profile spacing of 2.5 m.

3.1.3 | Hillfort Kouřim-sv. Jiří

The hillfort area had previously been investigated by detailed magnetometry survey during 2010–2012. Data were collected in a regular 1 × 0.25 m grid covering all parts of the hillfort, including the northern bailey, acropolis and the southern part (Křivánek, 2013, 2019a, 2019b). Spatial results from the magnetogram were used for efficient emplacement of ERT profiles. Within this study, only results from the vicinity of the prospected fortification line are presented.

The survey on this hillfort consisted of three parallel ERT profiles (P1–P3) with length of 71 m and electrode spacing of 1 m, using an IWS HD electrode array across the outer rampart within the active agricultural land. In addition, a single ERT profile (P4) was measured across a part of the outer rampart well preserved in a grove between fields, with length of 31 m and 1 m electrode spacing, and using three different electrode arrays: WS HD, IWS HD and DD HD (Figure 4).

3.2 | Effect of ERT field settings

3.2.1 | Type of electrode array

The selection of electrode array directly affects (i) horizontal–vertical resolution, (ii) data coverage, (iii) depth of investigation and (iv) sensitivity (e.g., Dahlin & Zhou, 2004). In archaeological applications, the WS and DD arrays are most commonly used in HD variants with additional measured points (Loke, 2020). The general purpose of the WS array is imaging of horizontal or quasi-horizontal layers. The depth range is about one fifth the maximum distance between current electrodes, while the resolution is rather ideal for investigation of shallow structures (Loke, 2020). WS offers one of the best depth determinations relative to the other arrays. One of its disadvantages is that WS, due to its specific geometry, does not spare any measurement time when used for multichannel acquisition. The reciprocal variant of WS known as IWS must then be used. Due to the switched current and potential electrodes, IWS tends to pick up more telluric noise and have possibly lower sensitivity at large potential electrode spacings than does regular WS array (Prins et al., 2018). The DD array excels in imaging of vertical structures, its depth range is about one fifth of the maximum current electrodes distance and it offers the highest resolution. DD is significantly limited by a rapid decrease of measured potential at large dipole distance, and it is prone to artificial electrical noise (Loke, 2020). DD can be used without any modifications for multichannel measurements, which is its strong advantage.

Our tests of the WS and IWS arrays found no significant difference between the two in the case of profile P4 across rampart at Kouřim-sv. Jiří (Figure 5a,b), but IWS in a five-channel measurement system is ∼3 times faster in data acquisition (not five times, because all five different electrode pairs cannot be used at the ends of arrays). The mentioned greater telluric noise or lower sensitivity at the large potential electrode spacings probably does not affect the relatively short profiles used in archaeological prospection. Results from DD (Figure 5c) do not differ very much from those of the two WS variants, but still some differences can be observed. Optionally, a high-definition inverse model combining two or more different arrays (e.g., Bharti et al., 2016) like WS and DD might also be used (Figure 5d), especially in a situation when the original resolution is not sufficient for distinguishing targets. Combining WS and DD data enhanced most of the anomalies due to higher sensitivity and resolution. In general, both ramparts and ditches usually form a horizontal layer (due to erosion, gravitational collapse or agricultural activities), and thus, WS/IWS arrays tend to be better for that layer's imaging.

3.2.2 | Selection of electrode spacing

Due to the different number of measured points, electrode spacing directly affects the method's resolution in both vertical and horizontal directions (Dahlin & Zhou, 2004). For example, a profile measured

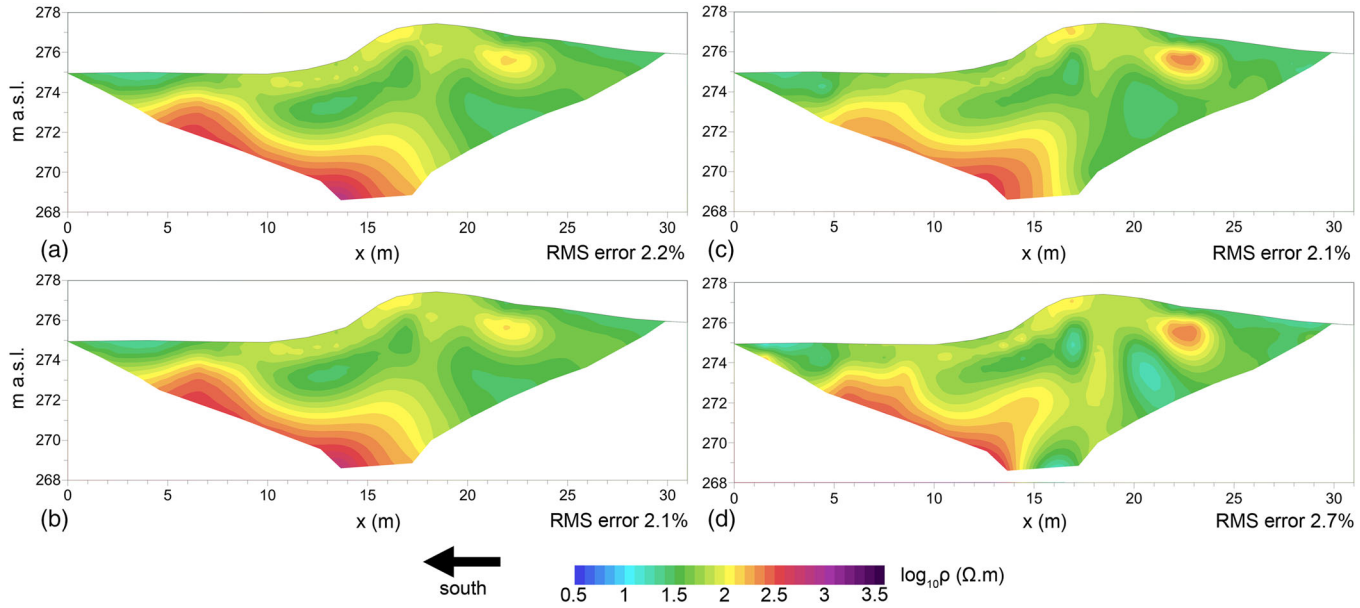

FIGURE 5 Inversion results for the different ERT arrays from Kouřim-sv. Jiří profile P4: (a) Wenner–Schlumberger, (b) inverse Wenner–Schlumberger, (c) dipole–dipole and (d) combined (concatenated) inversion of Wenner–Schlumberger and dipole–dipole [Colour figure can be viewed at wileyonlinelibrary.com]

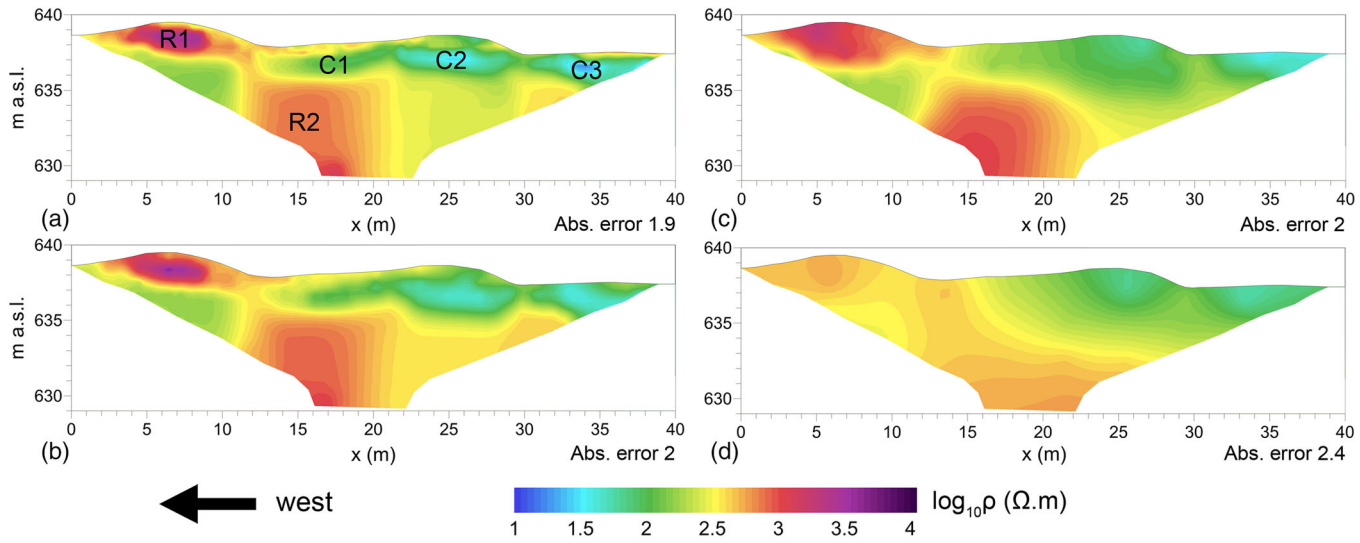

FIGURE 6 Comparison of inversion results from double inner rampart at hillfort Štěpánov, profile P3: (a) electrode spacing of 0.5 m, (b) electrode spacing of 1 m, (c) electrode spacing of 2 m and (d) electrode spacing of 4 m. High-resistivity (R) and low-resistivity structures (C) are described in Section 3.2.2 [Colour figure can be viewed at wileyonlinelibrary.com]

with 1 m electrode spacing will have roughly four times more points than does the same profile with 2 m electrode spacing, thus making the choice of proper electrode spacing very important. Depending on the targeted structures and desired resolution, small spacings of 0.25, 0.5 and 1.0 m are usually used in archaeology (e.g., Al-Saadi et al., 2017; Balkaya et al., 2018; Fernández-Álvarez et al., 2017). Because ramparts and ditches usually are of a size and are measured on a scale of metres, the electrode spacing of 1 m generally gives results with sufficient detail, but we investigated differences in resolution among various electrode spacings in the case of a double inner rampart at Štěpánov. Four different electrode spacings (0.5, 1, 2 and 4 m) were tested on the 40-m-long profile P3. The very dense electrode spacing of 0.5 m (Figure 6a) clearly identifies high-resistivity stones used in building a left rampart (R1) as well as volcanic basement (R2). Low-resistivity zones C1 and C3 probably represent remains of the former ditches. It is unclear why there is also a low-resistivity zone C2 under the right rampart, which manifests only slightly higher resistivity compared with the left rampart. The

geophysical image is practically unchanged in the case of electrode spacing of 1 m (Figure 6b), where only some minor changes near the surface can be observed compared with electrode spacing of 0.5 m. A different situation occurs in Figure 6c, where results from 2 m electrode spacing are displayed. The extent of the R1 structure is larger, and individual low-resistivity zones C1–C3 are merged into a single zone or are disappearing. The longest electrode spacing of 4 m (Figure 6d) loses the resolution and deforms the structures so that even the high-resistivity stones of R1 become nearly indistinguishable. The test proved that 1 m electrode spacing is adequate for surveying hillfort fortifications. Closer electrode spacing can be beneficial for imaging the internal structure of ramparts or ditches, while electrode spacings longer than 1 m are clearly losing the required resolution and should be avoided in the case of structures several metres in size.

4 | RESULTS

4.1 | Hillfort Štěpánov

Inverted ERT profile P1 (Figure 7a) shows an elevated structure of the rampart (position 23–32 m) with mid-range resistivity around 100 Ωm and a high-resistivity anomaly reaching 1000 Ωm on the eastern side (R1). Underneath the eastern side, there is a low-resistivity anomaly of 30 Ωm (C1a) to depth of ~2 m and width ~3 m. In addition, there is a second, similar anomaly on the eastern side of the rampart (C1b). The rest of the profile shows mid-range resistivity (100–300 Ωm, C2) with a varying thickness from 2 to 6 m under the surface and with deeper parts exhibiting higher resistivities from ~300 to 1000 Ωm (R2).

An inverted section from a double inner rampart (profile P2; Figure 7b) shows a rampart structure (position 12–40 m) with high resistivities reaching up to 10 000 Ωm (R3) and thickness from 1 to 3 m. Below the eastern side of both ramparts are low-resistivity anomalies of ~30 Ωm (C3) with 2 m thickness and 6 m width, both starting at 2 m below the surface. Around the rampart structure are small-scale high-resistivity anomalies (>1000 Ωm, R4) near the surface, while underneath lies a layer 4–5 m thick of mid-range resistivity around 100 Ωm (C4). Deeper parts of the profile are represented by high resistivity from 300 to 1000 Ωm (R5). Because the results from profile P3 are similar to those of profile P2, these results are only briefly described in Section 3.2.2.

4.2 | Hillfort Zámka

Magnetometry survey (vertical gradient) shows a positive, roughly north–south-oriented stripe anomaly in *x*-position range 30–50 m (A1), which turns on the south end towards the west (Figure 8). The

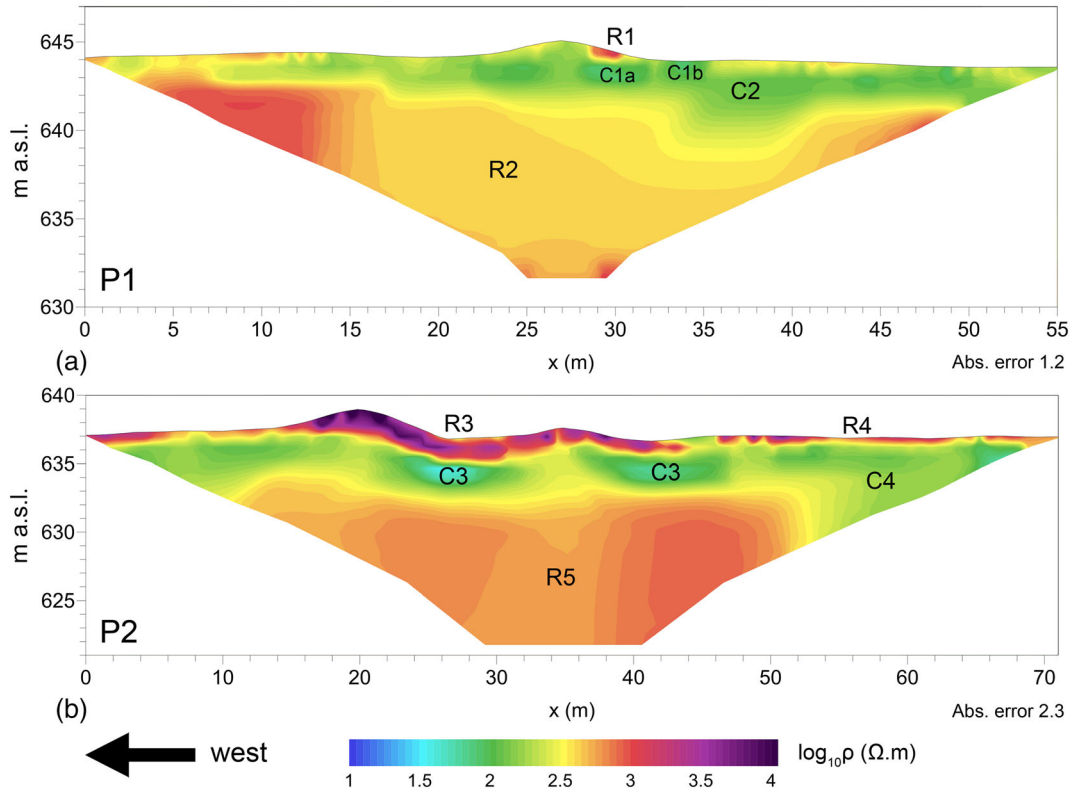

FIGURE 7 Inversion results for ERT profiles from hillfort Štěpánov: (a) profile P1 crossing outer rampart and (b) profile P2 crossing double inner rampart. High-resistivity structures R1 and R3 are related to ramparts, while low-resistivity anomalies C1 and C3 show possible remains of the ditches. Other marked structures indicate various lithologies (see Section 5.1.1) [Colour figure can be viewed at wileyonlinelibrary.com]

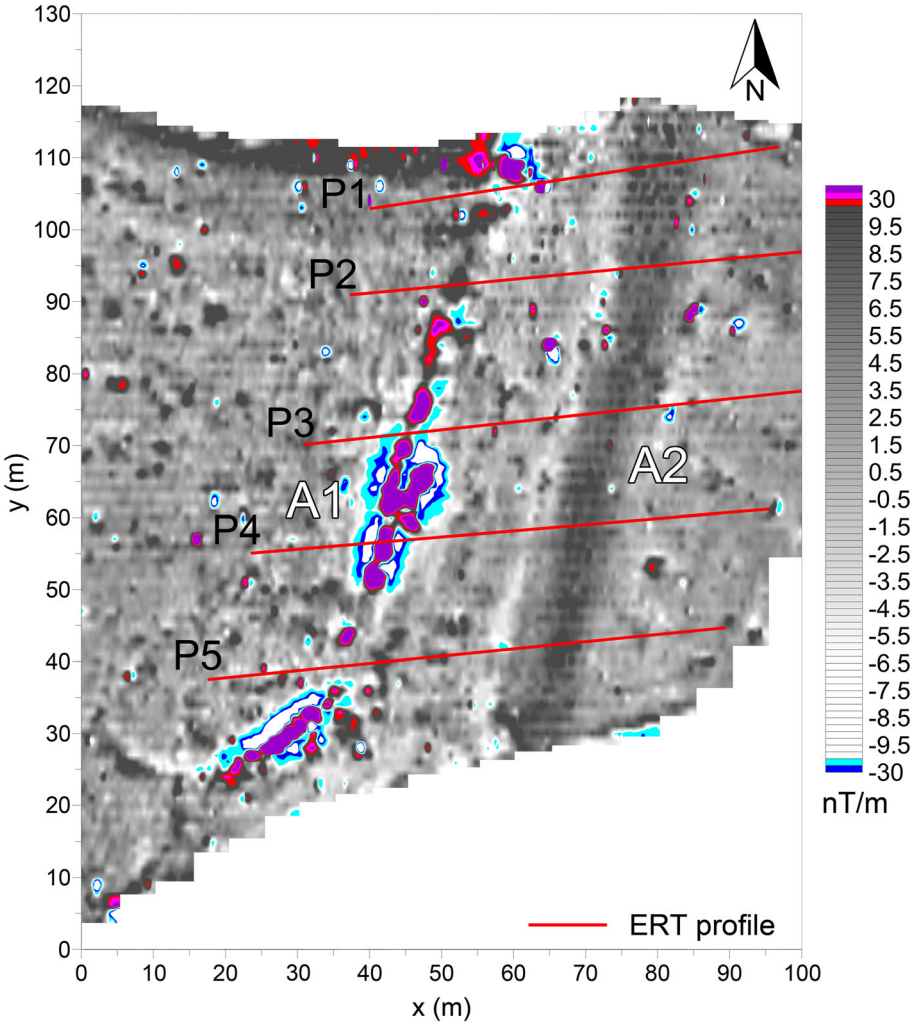

FIGURE 8 Interpolated results from the magnetometry survey within the hillfort Zámka with placement of ERT profiles. The strong anomaly A1 marks the rampart, while the uniform anomaly A2 represents the ditch [Colour figure can be viewed at wileyonlinelibrary.com]

anomaly has varying width locally exceeding ±30 nT. There is a second north–south-oriented stripe (A2) with more uniform distribution around +10 nT located between *x* positions 60 and 80 m. The remainder of the image is filled with local, small-scale and mostly positive anomalies.

Figure 9a–e shows inverted sections from all five ERT profiles (P1–P5) measured by WS HD array. At the beginning of profiles P1–P3 from positions 0 to 20–30 m, there is a high-resistivity layer between 130 and 600 Ωm (R1) with thickness of around 1–2 m. Below lies a low-resistivity layer of ∼30–50 Ωm with varying thickness from 4 to 8 m (C1). This layer is interrupted between positions 13 and 39 m by a more resistive anomaly of 100–300 Ωm (R2) protruding upwards on the P1 profile. On P2 and P3 profiles, a more resistive layer with values ranging from 100 to 1000 Ωm (R2) lies below the low-resistivity layer. The P4 profile can be characterized by high-resistivity values of 100–1000 Ωm (R3) from positions 0 to 40 m, with low-resistivity anomalies (∼50 Ωm, C2) placed between 4 and 10 m and at 20 m. The eastern side of the profile shows much lower resistivity around 50 Ωm (C3), with a small, high-resistivity anomaly (∼300 Ωm, R4) between 60 and 66 m. The P5 profile manifests generally high resistivities between 300 and 1000 Ωm (R5) from positions 0 to 42 m, while there are some smaller low-resistivity anomalies at 16 and 24 m (50 and 30 Ωm, respectively; C4). The rest of the profile to the east shows uniform resistivity around 50 Ωm (C5).

Figure 10 shows interpolated results depicted as integral values from top to a certain depth from the FDEM survey. The out-of-phase component (apparent resistivity, Figure 10a) generally exhibits low apparent resistivities between 30 and 90 Ωm within all three integral volumes, while only the SW corner shows higher resistivities up to 200 Ωm. Apparent resistivities rise gradually from shallow to greater depth, and a high-resistivity anomaly in the SW spreads with increasing depth. In Figure 10b, results from the in-phase component show distinct differences among individual integral volumes. From the top to depth about 1.1 m, there are two indistinct NNE–SSW-oriented anomalies (∼10 m wide) forming two stripes. Within integral values to a depth of about 2.1 m, both stripes are clearly visible with lower in-phase values compared with the surrounding environment, but the western stripe is stronger. Integral values to a depth of about 3.3 m show a narrower and more visible western stripe, due to higher in-phase values in the surrounding environment, while the eastern stripe has disappeared completely.

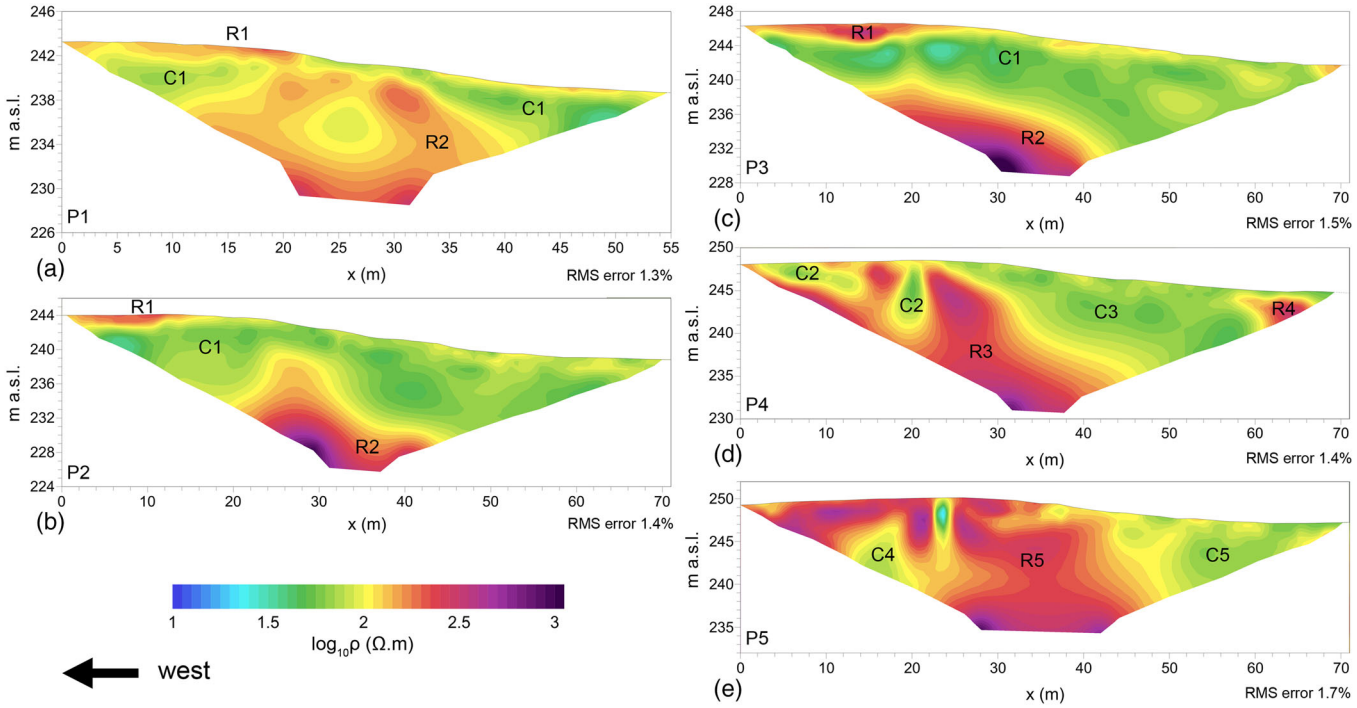

FIGURE 9 Inversion results for the ERT profiles P1–P5 (a–e) from the hillfort Zámka. High-resistivity structure R1 represents remains of the rampart, while all other marked anomalies can be related to soil and/or geological features (see Section 5.1.2). The ditch is completely invisible in the resistivity image [Colour figure can be viewed at wileyonlinelibrary.com]

4.3 | Hillfort Kouřim-sv. Jiří

Figure 11 displays interpolated results from the magnetometry survey, showing several elongated, mostly positive anomalies. The most significant anomalies are two east–west-oriented stripes between *x* positions 20 and 100 m (A1) followed by a perpendicular stripe trending to the north between *y* positions 0 and 60 m. A less distinct anomaly between *x* positions 40 and 120 m (A2) forms several positive and negative stripes coinciding with an elevated rise in the topography. At the east of the image, these stripes are followed by a more significant positive anomaly (A3).

Figure 12a–d shows inverted sections from all four ERT profiles (P1–P4) measured by IWS HD array. Three resistivity layers can be distinguished on the P1 profile: a top layer ~2 m thick with low resistivity around 30 Ωm (C1) and with a resistive anomaly around 100 Ωm between positions 44 and 52 m (R1), a mid-layer with thickness of ~5 m and almost uniform very low resistivity around 1 Ωm (C2), and a base layer with increasing resistivity from 100 to 1000 Ωm (R2). Profiles P2 and P3 are quite similar, with a low-resistivity layer of 30–80 Ωm ~1–2 m thick near the surface (C3). That thickness is increasing to 4 m from position 40 m on P2 and to 8 m at position 54 m on the P3 profile. The remainder of the profiles to the depth of 17 m exhibit high resistivity from 300 to 1500 Ωm (R3), while only between positions 30 and 44 m are lower resistivities ranging from 100 to 300 Ωm observed in the top 5 m and forming distinct mid-resistivity anomalies (R4). The P4 profile shows an elevated rampart structure at positions 10–21 m, with mid-resistivity between 60 and 100 Ωm to a depth of around 1.5 m (C4). The rest of the profile generally shows lower resistivities of ~30 Ωm (C5), with a higher resistive anomaly of 100 Ωm from 22 to 28 m ~2 m below the surface (R5). Between 5 and 15 m, a high-resistivity anomaly 100–300 Ωm (R6) is protruding from lower portions of the profile.

5 | DISCUSSION

5.1 | Geophysical interpretation

5.1.1 | Hillfort Štěpánov

Only the eastern side of the outer rampart on profile P1 (Figure 7a) with high resistivity (probably caused by piled up stones) is clearly visible within the elevated structure of the rampart (R1). The rest of the rampart has the same resistivity as the top geological layer, which can be related to weathered basaltic rocks and suggests a different construction of the outer rampart compared with that of the inner double rampart. Below the eastern side of the rampart there is a low-resistivity anomaly (C1a) that can possibly coincide with a former ditch, but we are aware that it might be an inversion artefact caused by compensation effects in the resistivity model. Due to this fact, it is possible that the former ditch is more likely represented by the C1b anomaly. It is certain that the rampart had a very different form during

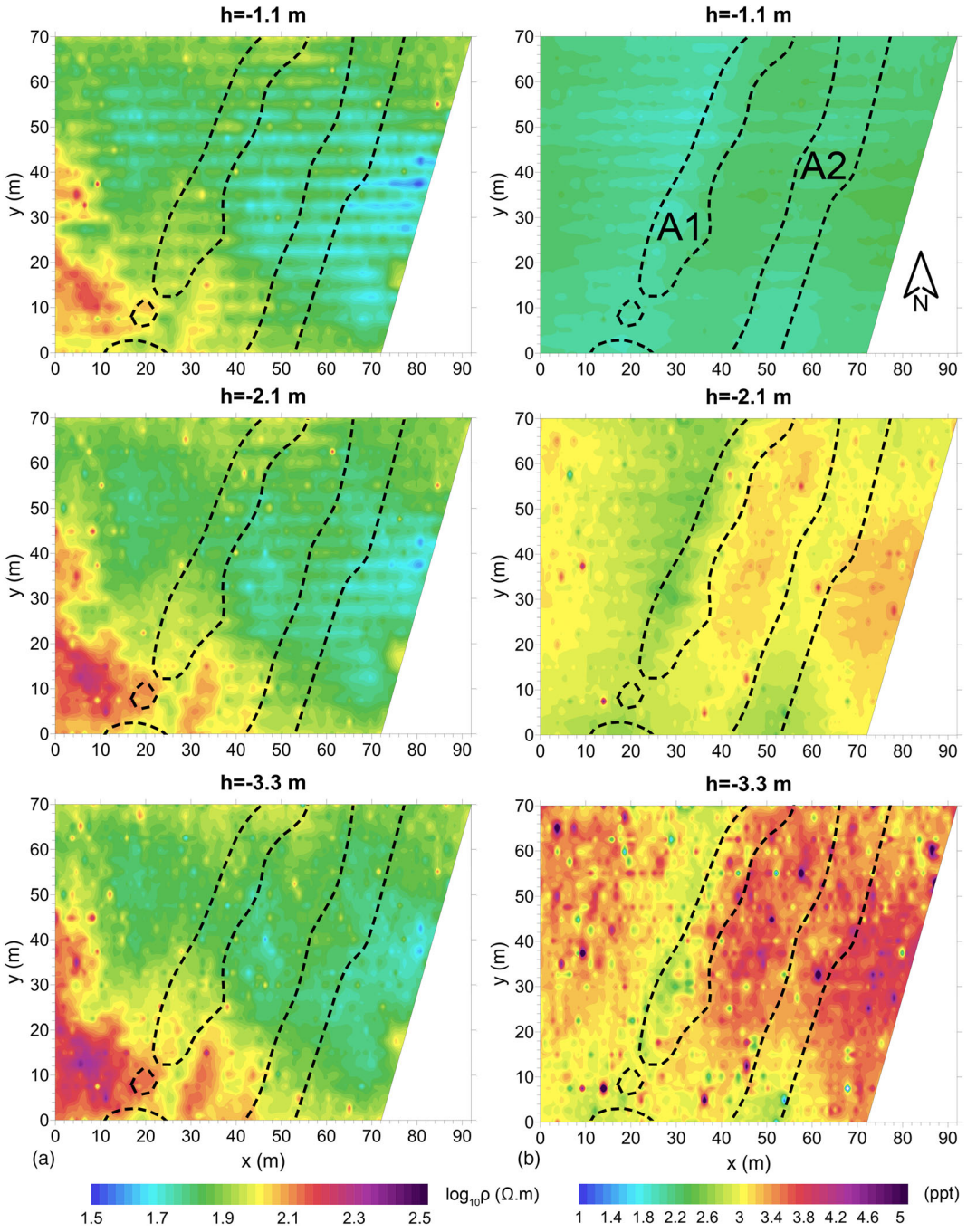

FIGURE 10 Electromagnetic survey results from the hillfort Zámka: (a) out-of-phase component (apparent resistivity) and (b) in-phase component (magnetic susceptibility); both for integrated values from top to depths of −1.1/−2.1/−3.3 m. Within images, the shapes (black broken line) of magnetic anomalies related to the rampart (A1) and the ditch (A2) are drawn [Colour figure can be viewed at wileyonlinelibrary.com]

the Bronze Age, so it is possible that through the years, the rampart collapsed to the sides and covered the ditch. The deepest portion of the profile is built of compact bedrock.

An inner double rampart on profile P2 (Figure 7b), stacked from stones, is much more visible due to extremely high-resistivity values (R3). Below the eastern side of both ramparts, there are low-resistivity anomalies (C3) that can probably be related to the filled ditches. The same can be said in the case of the outer rampart, where former rampart structures also possibly collapsed through the years to the sides and covered the ditches. The emplacement of C3 anomalies directly under the R3 high-resistivity anomaly raises the question whether these conductors are not caused by an inversion process, but, due to their strict location under the former ditches and not elsewhere under R3; we are not inclined to such explanation. The ramparts, same as the ditches, are clearly emerging from the weathered basaltic bedrock (C4) that is covering the compact basement (R5).

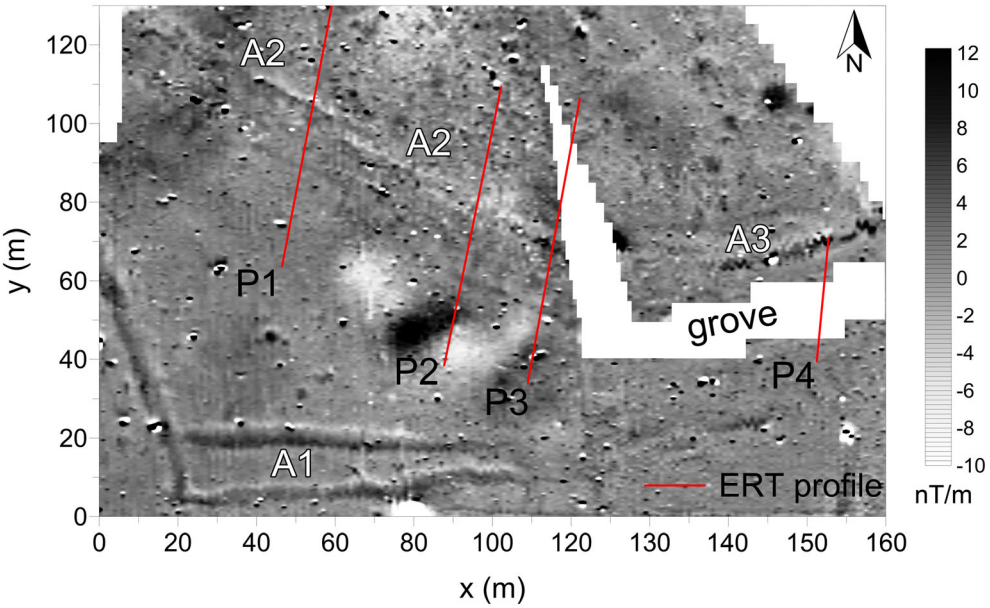

FIGURE 11 Interpolated results from magnetometry survey within hillfort Kouřim-sv. Jiří with placement of ERT profiles. Two positive anomalies (A1) probably represent the outer double ditch, while several stripe-like anomalies (A2) show ploughed remains of the rampart and ditches. The positive anomaly A3 can be related to the ditch behind the rampart hidden in a grove [Colour figure can be viewed at wileyonlinelibrary.com]

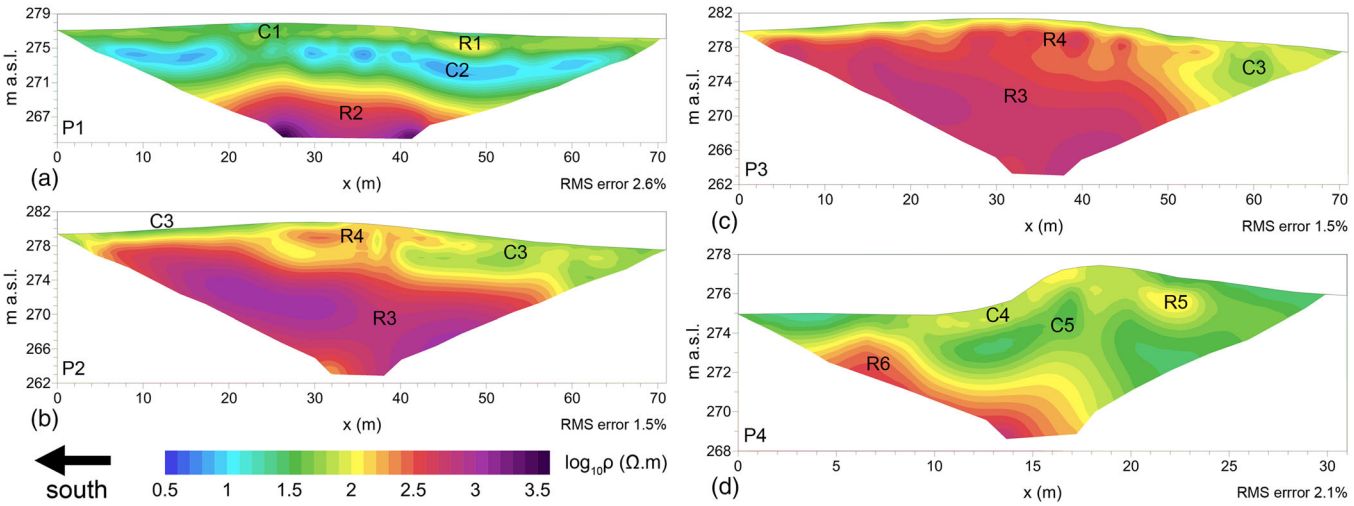

FIGURE 12 Inversion results for ERT profiles P1–P4 (a–d) from the hillfort Kouřim-sv. Jiří. High-resistivity anomalies R1 and R4 might represent ploughed remains of the rampart within the field, while the low-resistivity anomaly C4 can be related to a rampart in a grove. All other marked structures show various soil and/or geological features (see Section 5.1.3) [Colour figure can be viewed at wileyonlinelibrary.com]

5.1.2 | Hillfort Zámka

The fortification of the hillfort Zámka is not visible in the present topography, but it can be clearly distinguished with magnetics (Figure 8), where it is causing positive anomalies. The rampart (A1) was probably burned, thereby resulting in a strong positive anomaly, while infill of the ditch (A2) is a little bit different than the regular on-site soil, also presenting as a (weaker) positive anomaly.

The ERT results (Figure 9) only detect the stones, from which the rampart was built forming a high-resistivity layer (R1) at the beginning of profiles P1–P3. Due to agricultural activities and erosion of topsoil layers, in the present day, the stones are ploughed and spread to the inner upper flat area of the hillfort acropolis. A low-resistivity layer (C1, C3 and C5) within all profiles can be associated with the Quaternary loess cover, supported by an accumulation of topsoils in the depression. The high-resistivity structures on the bottom of P1–P3 (R2) and the western sides of P4/P5 (R3 and R5) are probably caused by the Proterozoic basement greywackes and siltstones, which especially on P4/P5 are moving to the surface due to a change in topography of the inner hillfort area.

Unfortunately, ERT was completely insensitive to the fill of the former ditch on all profiles, despite that it is highly visible in magnetic data. Because the magnetometry survey provided no vertical information, an FDEM survey was conducted to obtain it. The out-of-phase component (related to apparent resistivity) proves (Figure 10a) that the ditch has no inductive response differing from the surrounding loess and soil cover within all three depth levels. The shapes of magnetic anomalies for both rampart and ditch drawn

to the resistivity slices have no relation to the measured resistivity structures. A different situation occurs in the in-phase component (related to magnetic susceptibility and thus to magnetic properties; Figure 10b), where distinct stripe-like anomalies can be seen coinciding with the shape of fortification structures from the magnetometry survey. Integral values to a depth of about 1.1 m show lower in-phase values that can be assigned to the rampart and ditch while the rampart is significantly stretched in the east–west direction. Within integral values to a depth of about 2.1 m, the in-phase contrast is more evident, especially for the rampart, but both fortification structures have lower in-phase values than the surrounding environment. Integral values to a depth of about 3.3 m show that the rampart is narrowing in the in-phase image and moves a little to the west compared with the shape from magnetics. The ditch is disappearing completely.

5.1.3 | Hillfort Kouřim-sv. Jiří

Fortifications within the open and active agricultural field are almost invisible in the present topography. The results from magnetics (Figure 11) confirmed ploughed out remains of the original southern rampart of the acropolis with different outer ditches (A2; Křivánek, 2019a, 2019b). Other fortification lines can be seen on the magnetogram as positive anomalies: A1 probably represents an outer double ditch, with possible remains of the rampart; A3, which can be related to a ditch, is surprisingly situated behind the well-preserved rampart in the grove.

The ERT results on the P1–P3 profiles are clearly affected by agricultural activities (Figure 12). On P1 only, small near-surface anomalies to depth of about 2 m between positions 34 and 50 m with a little bit higher resistivity (R1) can possibly be attributed to material of a former rampart that has been ploughed out. A low-resistivity layer (C2) underneath can be associated with aeolian sediments (loess), while bedrock with crystalline rocks (migmatites and/or orthogneisses) is indicated by high resistivity (R2). P2 and P3 appear similarly, but on both profiles, resistive crystalline rocks (R3) are rising up to near the surface while the sedimentary cover is thickened only to 1–2 m (C3). Only on the northern edges of the profiles do the aeolian sediments have greater thickness around 6 m. Between positions 26 and 42 m at the depth of the first several metres, there are several anomalies with lower resistivity (R4) within the crystalline basement on both profiles. These may be related to the former rampart. Results from P4 across a well-preserved part of the rampart in the grove prove that the rampart was not built of stones at all, but interpretation of P4 is somehow difficult due to low-resistivity contrast and possible inversion artefacts, especially represented by pairs of anomalies C4/C5 and R5/C5. The rampart can possibly be characterized by mid-resistivity values (C4) to depth around 2 m and which are slightly greater than the surrounding sediments (C5) but still too low for piled up stones when compared with other investigated hillforts having clear stone ramparts. At the beginning of the profile, crystalline rocks (R6) are rising from below. At the end of the profile, behind the rampart, there are no signs of the ditch discovered by the magnetometry survey (A3 in the magnetogram).

5.2 | Effects of preservation of fortification, building material and bedrock type

For successful identification of the fortification, a resistivity contrast between the fortification structure and surrounding soil and/or rock is most important. This is generally most affected by present-day preservation of the rampart, the building material used and the bedrock type. As can be seen in the examples from Štěpánov, well-preserved stony ramparts can be successfully identified with ERT even on rocky bedrock. Ramparts of piled up stones usually exhibit only weak interconnection between individual stones, thus resulting in exceptional high resistivity. A completely different situation exists at Kouřim-sv. Jiří, where only earthen ramparts were built. Even a quite well-preserved part of the rampart in the grove is only scarcely distinguishable from the bedrock in the resistivity image. The poorest results were achieved on active agricultural fields with noticeably destroyed ramparts. The potential of ERT applications is very limited in this case due to mixing of the rampart material with the on-site soils. If the rampart had been built of stones, ERT could find at least some remnants, as at Zámka, but in the case of earthen ramparts, as probably was the case at Kouřim-sv. Jiří, ERT is most likely unable to see any resistivity contrast.

The bedrock type mostly affects the identification of ditches. The strongest resistivity contrast can be found at localities where ditches were carved directly into rocky bedrock. Even if it was more recently filled with a rocky-and-sedimentary mixture, the ditch holds moisture better in comparison with the surrounding rocks, as it is more porous, is less compacted and acts as a kind of drainage channel. Thus, it exhibits as a low-resistivity zone. This is the case of Štěpánov, where low-resistivity zones can be found on the outer side of each rampart. In the case of Zámka, where the ditch was built inside the aeolian sediments and is nicely seen in magnetic data, ERT completely failed. As the ditch was probably filled with a similar material (i.e., on-site soil and loess), the resistivity contrast is almost negligible. That was also proven by an additional FDEM survey using a different physical method (electromagnetic induction) for obtaining the resistivity information. The ditch was completely invisible within the out-of-phase component (apparent resistivity), but it was identifiable by in-phase (magnetic susceptibility). This means that the ditch at Zámka formed a layer with different magnetic susceptibility but the same resistivity as the surrounding environment. On accessible sites with strong magnetic anomalies caused by ditches, therefore, FDEM survey can be used satisfactorily instead of ERT for obtaining vertical information.

5.3 | Impact of agricultural activities

Within the cultivated fields, where arable soil plays the main role in agricultural activities, usually the top 0.2–0.4 m of the soil is affected

by ploughing. The ploughing causes soil loss and can rapidly and irreparably damage archaeological sites (e.g., Lambrick, 2004; Noble et al., 2019). This occurs due to increased alteration of the soil chemistry and aeration of the soil, as well as to compaction and fragmentation by farm machinery (e.g., Dain-Owens et al., 2013; Kibblewhite et al., 2015). Ploughing also leads to displacements of archaeological artefacts and objects (e.g., Yorston et al., 1990).

Ploughing affects not only small archaeological artefacts but also such large-scale structures such as ramparts and ditches (e.g., Cruz et al., 2008; Zhurbin & Borisov, 2020). The building material of ramparts or material filling ditches is ploughed to the sides, deforming the shape of former fortifications, destroying their elevation profile and reducing thickness of the archaeological layers preserved in situ in the subsoil. This can be seen at the Zámka and Kouřim-sv. Jiří sites, where remnants of fortifications are located within active or recently active agricultural land. The ramparts at both sites emerge from fields today only in the form of indistinct terrain rises. In this case, ERT is only able to identify rampart building materials that are displaced to the sides. At Zámka, a stony layer can be clearly identified even when mixed with on-site soil. The quantity of the displacement is clearly visible in an in-phase component from the FDEM survey (Figure 10b) within integral values to depths of 1.1 and 2.1 m. It is very unlikely that ploughing would also affect the third layer. A discrepancy between rampart shapes from the magnetometry survey and integral values of in-phase from top to depth of 3.3 m obtained by FDEM survey is probably caused mainly by natural factors and different depth sensitivities of the two methods. At Kouřim-sv. Jiří, where the rampart was made of earth, ERT cannot identify any remnants of the rampart due to mixing of the rampart building material with on-site soils, both of which have similar resistivity.

6 | CONCLUSION

ERT was used to survey hillfort fortifications at three localities within the Czech Republic characterized by different (i) ages (from the Bronze Age to early medieval), (ii) bedrock types, (iii) present-day conditions and (iv) effects of agricultural activities. Generally, the results show that ERT is highly suitable for mapping well-preserved stony ramparts or ditches carved into rocky bedrock and offering a huge resistivity contrast. The method is also applicable for describing the internal structure of earthen ramparts if they were preserved and not destroyed by human activities. A substantially poorer situation was seen in the cases of hillforts located on agricultural lands, where ramparts and ditches had been affected by ploughing. Under such conditions, ERT is able to find only remnants of former ramparts (if they were stacked of stones), while ditches are almost completely invisible due to mixing of ditch infills with on-site soils and thus resulting in no resistivity contrast. Still, ERT is a valuable technique capable of obtaining depth information and for mapping an internal structure of fortifications that can be carried out under difficult conditions that include rocky and heavily forested sites. The information thereby obtained can significantly improve our understanding concerning the functions of a hillfort, its former environmental conditions, its original inhabitants, relevant human–environmental interactions and/or the state of the archaeological site's subsurface preservation.

ACKNOWLEDGEMENTS

This work was supported by the INTER-EXCELLENCE programme of the Ministry of Education, Youth and Sports of the Czech Republic (MEYS; Ministerstvo Školství, Mládeže a Tělovýchovy), Grant No. LTC19029, and with institutional support from the Centre for Geosphere Dynamics, Charles University (Univerzita Karlova v Praze) (UNCE/SCI/006). The authors are very grateful to the associate editor Dr. Eileen Ernenwein and two anonymous reviewers for valuable comments that have improved the manuscript.

CONFLICT OF INTERESTS

Conflict of interest is not applicable to this work.

DATA AVAILABILITY STATEMENT

All geophysical data presented here are available in standard industry formats from https://doi.org/10.17632/wt4szt427g.1.

ORCID

Radek Klanica https://orcid.org/0000-0002-8302-7537
Roman Křivánek https://orcid.org/0000-0003-1878-7748
Hana Grison https://orcid.org/0000-0002-0402-2026
Petr Tábořík https://orcid.org/0000-0002-5159-7703

REFERENCES

Al-Saadi, O. S., Schmidt, V., Becken, M., & Fritsch, T. (2017). Very-high-resolution electrical resistivity imaging of buried foundations of a Roman villa near Nonnweiler, Germany. *Archaeological Prospection*, *25*, 1–10. https://doi.org/10.1002/arp.1703

Andreou, G. M., Opits, R., Manning, S. W., Fisher, K. D., Sewell, D. A., Georgiou, A., & Urban, T. (2017). Integrated methods for understanding and monitoring the loss of coastal archaeological sites: The case of Tochni-Lakkia, south-central Cyprus. *Journal of Archaeological Science: Reports*, *12*, 197–208. https://doi.org/10.1016/j.jasrep.2017.01.025

Balkaya, C., Kalyoncuoğlu, Ü. Y., Özhanlı, M., Merter, G., Çakmak, O., & Güven, İ. T. (2018). Ground-penetrating radar and electrical resistivity tomography studies in the biblical Pisidian Antioch city, southwest Anatolia. *Archaeological Prospection*, *25*, 285–300. https://doi.org/10.1002/arp.1708

Bharti, A. K., Pal, S. K., Priyam, P., Pathak, V. K., Kumar, R., & Ranjan, S. K. (2016). Detection of illegal mine voids using electrical resistivity tomography: The case-study of Raniganj coalfield (India). *Engineering Geology*, *213*, 120–132. https://doi.org/10.1016/j.enggeo.2016.09.004

Cajz, V. (2000). Proposal of lithostratigraphy for the České středohoří Mts. volcanics. *Věstník Českého geologického ústavu*, *75*(1), 7–16.

Catanzariti, G., McIntosh, G., Soares, A. M. M., Díaz-Martínez, E., Kresten, P., & Osete, M. L. (2008). Archaeomagnetic dating of a vitrified wall at the Late Bronze Age settlement of Misericordia (Serpa, Portugal). *Journal of Archaeological Science*, *35*, 1399–1407. https://doi.org/10.1016/j.jas.2007.10.004

Christensen, J. (2004). Warfare in the European Neolithic. *Acta Archaeologica*, *75*, 129–156. https://doi.org/10.1111/j.0065-001X.2004.00014.x

Cruz, F., Petit, C., Pertlwieser, T., Chaume, B., Mordant, C., & Chateau, C. (2008). Erosion of the defensive system of the 'princely' site of Vix

(France): A geoarchaeological approach. In E. Meylemans, J. Poesen, & I. In't Ven (Eds.), *The Archaeology of Erosion, the Erosion of Archaeology. Proceedings of the Brussels Conference*. Brussels: Flanders Heritage Agency.

Čtverák, V., Lutovský, M., Slabina, M., & Smejtek, L. (2003). *Encyklopedie hradišťv Čechách*. Libri.

CUZK. (2017). Digital Terrain Model of the Czech Republic of the 5th generation (DMR 5G). https://ags.cuzk.cz/av/

Dahlin, T., & Zhou, B. (2004). A numerical comparison of 2D resistivity imaging with 10 electrode arrays. *Geophysical Prospecting*, *52*, 379–398. https://doi.org/10.1111/j.1365-2478.2004.00423.x

Dain-Owens, A., Kibblewhite, M., Hann, M., & Godwin, R. (2013). The risk of harm to archaeological artefacts in soil from dynamic subsurface pressures generated by agricultural operations: Experimental studies. *Archaeometry*, *55*(6), 1175–1186. https://doi.org/10.1111/j.1475-4754.2012.00720.x

de Jong, S. M., Heijenk, R. A., Nijland, W., & van der Meijde, M. (2020). Monitoring soil moisture dynamics using electrical resistivity tomography under homogeneous field conditions. *Sensors*, *20*(18), 1–18. https://doi.org/10.3390/s20185313

de Smedt, P., van Meirvenne, M., Herremans, D., de Reu, J., Saey, T., Meerschman, E., Crombé, P., & de Clercq, W. (2013). The 3-D reconstruction of medieval wetland reclamation through electromagnetic induction survey. *Scientific Reports*, *3*, 1–5. https://doi.org/10.1038/srep01517

Di Maio, R., La Manna, M., Piegari, E., Zara, A., & Bonetto, J. (2018). Reconstruction of a Mediterranean coast archaeological site by integration of geophysical and archaeological data: The eastern district of the ancient city of Nora (Sardinia, Italy). *Journal of Archaeological Science: Reports*, *20*, 230–238. https://doi.org/10.1016/j.jasrep.2018.05.003

Fassbinder, J. W. E. (2017). Magnetometry for archaeology. In A. S. Gilbert (Ed.), *Encyclopedia of geoarchaeology*. Springer Science+Business Media Dordrecht. https://doi.org/10.1007/978-1-4020-4409-0_169

Fassbinder, J. W. E., & Stanjek, H. (1993). Occurrence of bacterial magnetite in soils from archaeological sites. *Archaeologia Polonia*, *31*, 117–128.

Fernández-Álvarez, J. P., Rubio-Melendi, D., Castillo, J. A. Q., González-Quirós, A., & Cimadevilla-Fuente, D. (2017). Combined GPR and ERT exploratory geophysical survey of the Medieval Village of Pancorbo Castle (Burgos, Spain). *Journal of Applied Geophysics*, *144*, 86–93. https://doi.org/10.1016/j.jappgeo.2017.07.002

Goodman, D., & Piro, S. (2013). *GPR remote sensing in archaeology*. Springer.

Hegyi, A., Urdea, P., Floca, C., Ardelean, A., & Onaca, A. (2018). Mapping the subsurface structures of a lost medieval village in South-Western Romania by combining conventional geophysical methods. *Archaeological Prospection*, *26*, 21–32. https://doi.org/10.1002/arp.1720

Kibblewhite, M., Tóth, G., & Hermann, T. (2015). Predicting the preservation of cultural artefacts and buried materials in soil. *Science of the Total Environment*, *529*, 249–263. https://doi.org/10.1016/j.scitotenv.2015.04.036

Křivánek, R. (2008). Nové výsledky geofyzikálních průzkumů v širším areálu pravěkého a raně středověkého hradiště Zámka v Praze-Bohnicích. *Archaeologica Pragensia*, *19*, 233–256.

Křivánek, R. (2010). Geofyzikální průzkum hradišť Přerovská hůra a Zámka ohrožených stavebním záměrem. *Archeologické Rozhledy*, *LXII*(3), 480–491.

Křivánek, R. (2013). Changes of structure and extent of early medieval strongholds in Central Bohemia from geophysical surveys of sites. Archaeological prospection. In W. Neubauer, I. Trinks, R. B. Salisbury, & C. H. Einwögerer (Eds.), *Proceedings of the 10th International Conference on Archaeological Prospection, Vienna, Austria, 29 May–2 June 2013* (pp. 281–284). Austrian Academy of Sciences Press.

Křivánek, R. (2019a). Přehled geofyzikálních průzkumů raně středověkých hradišť v Čechách: přínos, omezení, perspektivy (Overview of geophysical surveys of early medieval hillforts in Bohemia: Contribution, limitations, perspectives). In K. Chrzan, S. Mozdzioch, & S. Rodak (Eds.), *Współczesne metody badań wczesnośredniowiecznych grodów Europy Środkowo-Wschodniej* (pp. 145–154). IAE PAN.

Křivánek, R. (2019b). Fortified sites in Bohemian archaeology from the view of application of non-destructive geophysical methods. In *Zbornik Instituta za arheologiju, Serta instituti Archaeologici, Knjiga/Volume 13 (Fortifications, defence systems, structures and features in the past—Fortifikacije, obrambeni sustavi I structure u prošlosti, 4th International Conference of Mediaeval Archaeology—4. međunarodni znanstveni skup srednjovjekovne arheologije)* (pp. 55–62). Institute of Archaeology—Institut za arheologiju.

Kudrnáč, J. (1963). Vývoj slovanského osídlení mezi pražským Povltavím, Labem, Sázavou a Výrovkou. *Památky archeologické*, *54*, 173–221.

Lambrick, G. (2004). The management of archaeological sites in arable landscapes. In M. Corfield, P. Hinton, T. Nixon, & M. Pollard (Eds.), *Preserving archaeological remains in situ? Proceedings of the 2nd Conference 12–14 September 2001* (pp. 168–173). Museum of London Archaeology Service.

Le Borgne, E. (1960). Influence of fire on the magnetic properties of soil, of schist, and of granite. *Annales de Geographie*, *16*, 159–196.

Leontarakis, K., & Apostolopoulos, G. V. (2013). Model Stacking (MOST) technique applied in cross-hole ERT field data for the detection of Thessaloniki ancient walls' depth. *Journal of Applied Geophysics*, *93*, 101–113. https://doi.org/10.1016/j.jappgeo.2013.04.004

Loke, M. H. (2020). Rapid 2-D resistivity & IP inversion using the least-squares method. RES2DINV User's Manual, Geotomo Software. http://www.geotomosoft.com/

Loke, M. H., Acworth, I., & Dahlin, T. (2003). A comparison of smooth and blocky inversion methods in 2-D electrical imaging surveys. *Exploration Geophysics*, *34*, 182–187. https://doi.org/10.1071/EG03182

Loke, M. H., & Barker, R. D. (1996). Rapid least-squares inversion of apparent resistivity pseudosections by a quasi-Newton method. *Geophysical Prospecting*, *44*, 131–152. https://doi.org/10.1111/j.1365-2478.1996.tb00142.x

Mašek, N., & Fridrichová, M. (1965). Výzkum hradiště Zámka u Bohnic. In *Pražský sborník historický* (pp. 129–130). Archiv hlavního města Prahy, Praha.

Mullins, C. E. (1977). Magnetic susceptibility of the soil and its significance in soil science—A review. *Journal of Soil Science*, *28*, 223–246. https://doi.org/10.1111/j.1365-2389.1977.tb02232.x

Nero, C., Aning, A. A., Danuor, S. K., & Noye, R. M. (2016). Delineation of graves using electrical resistivity tomography. *Journal of Applied Geophysics*, *126*, 138–147. https://doi.org/10.1016/j.jappgeo.2016.01.012

Noble, G., Lamont, P., & Masson-Maclean, E. (2019). Assessing the ploughzone: The impact of cultivation on artefact survival and the cost/benefits of topsoil stripping prior to excavation. *Journal of Archaeological Science: Reports*, *23*, 549–558. https://doi.org/10.1016/j.jasrep.2018.11.015

Nowaczinski, E., Schukraft, G., Hecht, S., Rassmann, K., Bubenzer, O., & Eitel, B. (2012). A multimethodological approach for the investigation of archaeological ditches—Exemplified by the Early Bronze Age settlement of Fidvár Near Vráble (Slovakia). *Archaeological Prospection*, *19*, 281–295. https://doi.org/10.1002/arp.1434

Oliva, M. (2004). Flint mining, rondels, hillforts… Symbolic works or too much free time? *Archeologické rozhledy*, *56*, 499–531.

Osgood, R., Monks, S., & Toms, J. (2000). *Bronze Age warfare*. J.H. Haynes.

Oswin, J. (2009). *A field guide to geophysics in archaeology*. Springer-Verlag.

Parkinson, W. A., & Duffy, P. R. (2007). Fortifications and enclosures in European prehistory: A cross-cultural perspective. *Journal of Archaeological Research*, *15*, 97–141. https://doi.org/10.1007/s10814-007-9010-2

Prins, C., Thuro, K., & Krautblatter, M. (2018). The effectiveness of an inverse Wenner-Schlumberger array for geoelectrical karst

reconnaissance, on the Swabian Alb high plain, new line Wendlingen–Ulm, southwestern Germany. In *IAEG/AEG Annual Meeting Proceedings, San Francisco, California, 2018* (Vol. 3). Switzerland: Springer Nature.

Profantová, N. (1996). Slovanské osídlení hradiště Bohnice-Zámka a jeho zázemí: na základě výzkumů N. Maška. *Archaeologica Pragensia*, *12*, 65–140.

Rodrigues, S. I., Porsani, L. J., Santos, V. R. N., Deblais, P. A. D., & Giannini, P. C. F. (2009). GPR and inductive electromagnetic surveys applied in three coastal *sambaqui* (shell mounds) archaeological sites in Santa Catarina state, South Brazil. *Journal of Archaeological Science*, *36*, 2081–2088. https://doi.org/10.1016/j.jas.2009.05.013

Schultze, V., Linzen, S., Schüler, T., Chwala, A., Stolz, R., Schulz, M., & Meyer, H.-G. (2008). Rapid and sensitive magnetometer surveys of large areas using SQUIDs—The measurement system and its application to the Niederzimmern Neolithic double-ring ditch exploration. *Archaeological Prospection*, *15*, 113–131. https://doi.org/10.1002/arp.328

Simpson, D., Van Meirvenne, M., Lück, E., Bourgeois, J., & Rühlmann, J. (2010). Prospection of two circular Bronze Age ditches with multi-receiver electrical conductivity sensors (North Belgium). *Journal of Archaeological Science*, *37*, 2198–2206. https://doi.org/10.1016/j.jas.2010.03.017

Smrž, Z. (1995). Höhenlokalitäten der Knovízer Kultur in NW-Böhmen. *Památky archeologické*, *86*, 38–80.

Šolle, M. (1969). Kouřim v mladší a pozdní době hradištní. *Památky archeologické*, *60*, 1–124.

Šolle, M. (1993). Přemyslovská a děpoltická Kouřim podle výzkumu z let 1967–1977. *Archeologické rozhledy*, *45*, 268–278.

Šolle, M. (2000). *Po stopách přemyslovských Děpolticů: příspěvek ke genezi města Kouřimě*.

Tabbagh, A. (2017). Electrical resistivity and electromagnetism. In A. S. Gilbert (Ed.), *Encyclopedia of geoarchaeology*. Springer Science+Business Media Dordrecht. https://doi.org/10.1007/978-1-4020-4409-0_164

Tomanová, P. (2012). Kouřim—St.Georg. Přemyslid Administrative Centre and archaeology of the early medieval central places (strategies and methods). Diploma Thesis. Faculty of Arts, Charles University.

Urban, T. M., Rasic, J. T., Alix, C., Anderson, D. D., Chisholm, L., Jacob, R. W., Manning, S. W., Mason, O. K., Tremayne, A. H., & Vinson, D. (2019). Magnetic detection of archaeological hearths in Alaska: A tool for investigating the full span of human presence at the gateway to North America. *Quaternary Science Reviews*, *211*, 73–92. https://doi.org/10.1016/j.quascirev.2019.03.018

Urban, T. M., Vella, C., Bocancea, E., Tuttle, C. A., & Alcock, S. E. (2014). A geophysical investigation of a newly discovered Early Bronze Age site near Petra, Jordan. *Journal of Archaeological Science*, *42*, 260–272. https://doi.org/10.1016/j.jas.2013.11.017

Vencl, S. (1984). *Otázky poznání vojenství v archeologii. Archeologické studijní materiály 14*. Praha: Archeologický ústav ČSAV.

Wiseman, J., & El-Baz, F. (2007). *Remote sensing in archaeology*. Springer-Verlag.

Yorston, R. M., Gaffney, V. L., & Reynolds, P. J. (1990). Simulation of artefact movement due to cultivation. *Journal of Archaeological Science*, *17*(1), 67–83. https://doi.org/10.1016/0305-4403(90)90015-W

Zhao, W., Tian, G., Lin, Q., Wang, X., Wang, Y., & Bie, K. (2019). Integrated characterization of ancient burial mounds using ERT and limited drillings at the Hepu Han Tombs, in coastal area of Southern China. *Journal of Archaeological Science: Reports*, *23*, 617–625. https://doi.org/10.1016/j.jasrep.2018.11.016

Zhurbin, I. V., & Borisov, A. V. (2020). Non-destructive approach for studying medieval settlements destroyed by ploughing: Combining aerial photography, geophysical and soil surveys. *Archaeological Prospection*, *27*, 1–18. https://doi.org/10.1002/arp.1778

Zotti, G., & Neubauer, W. (2011). Astronomical aspects of *Kreisgrabenanlagen* (Neolithic circular ditch systems)—an interdisciplinary approach. *Proceedings of the International Astronomical Union*, *7*(S278), 349–356. https://doi.org/10.1017/S1743921311012798

How to cite this article: Klanica, R., Křivánek, R., Grison, H., Tábořík, P., & Šteffl, J. (2022). Capabilities and limitations of electrical resistivity tomography for mapping and surveying hillfort fortifications. *Archaeological Prospection*, 1–16. https://doi.org/10.1002/arp.1857